



LA-UR-02-6247
February 2003

Radiation Effects Studies in Transmutation Fuel Matrix/ Diluent Materials: FY02

Radiation Effects Studies in Transmutation Fuel Matrix/Diluent Materials: FY02

K.E. Sickafus, G. Egeland, and J.A. Valdez

*Materials Science and Technology Division, Los Alamos National
Laboratory, Mail stop G755, Los Alamos, NM 87545*

Summary

In FY02, the Radiation Effects and Characterization Team performed high energy, heavy ion irradiations on polycrystalline samples of ZrN to assess the radiation damage integrity of this nitride compound. We determined that the cubic crystalline phase of ZrN is stable against radiation induced transformations to significant radiation doses (collisional damage equivalent to approximately 200 displacements per lattice atom). These results are significant because they suggest that a ZrN fuel matrix will not succumb to amorphization or other phase transformations during service. Such transformations are usually accompanied by substantial volume changes and so, are detrimental to fuel integrity.

We also observed point defect hardening in ion irradiated ZrN. Using nanoindentation mechanical testing methods, we found that the hardness (H) of ZrN increases by $\sim 13\%$ upon irradiation with Xe ions to a peak displacement damage level equivalent to ~ 8 displacements per atom. At this damage level the hardness of ZrN was observed to increase from approximately $H = 24$ to $H = 27.5$ GPa. Interestingly, the Young's modulus (E) remained unchanged at this ion dose, with a measured value between 370-380 GPa, in good agreement with the value reported in the literature, $E = 380$ GPa. These results will help us to quantify the rate of embrittlement of ZrN during use (increase in H versus irradiation dose), while the results also reconfirm that the intrinsic structure of ZrN is unaffected by irradiation (E constant).

At high fluences of Xe, Kr, and He ion implantation (corresponding to a peak implantation concentration of up to $\sim 12.5\%$ Xe), we observed small bubbles (~ 10 nm diameter) in the irradiated microstructure that probably contain evolved Xe. This is significant because it indicates that at high fuel burn-ups, fission products such as Xe are likely to migrate either out of a ZrN matrix fuel or into voids in the microstructure. These fission product release mechanisms are detrimental to fuel performance.

NiAl is a candidate metal matrix for a dispersion fuel because of its high thermal conductivity. However, it is important to consider the radiation tolerance of this intermetallic compound. Therefore, we initiated an investigation of radiation damage effects in single crystal NiAl using ion implantation followed by ion beam channeling analysis to assess the rate of radiation damage accumulation in NiAl.

Finally, in a collaboration with the Institute for Transuranium Elements (ITU) in Karlsruhe, Germany, we are performing He desorption measurements on ZrN. These experiments will show the implications of temperature vs. evolution rate of He with various amounts of irradiation damage.

Zirconium Mononitride (ZrN)

Assessment of Radiation Tolerance

Various techniques have been used to evaluate the radiation damage under heavy ions and fission product implantation in ZrN. Using both cross-section and plan view

transmission electron microscopy (TEM) samples, irradiation damage from Xe and He ion implantation (300 KeV and 50 KeV respectively, both at 5×10^{16} fluence) has been characterized. Surface topography characterizations, using scanning electron microscopy (SEM), and atomic force microscopy (AFM), have been used to examine for the possibility of swelling effects due to inert gas implantations. The presence of implanted Xe gas was confirmed using energy dispersive spectrometry (EDS).

High Density Sample Preparation

For irradiation damage studies of zirconium nitride (ZrN), we require highly dense samples with surfaces polished to produce very low surface roughness. To achieve this goal, we produced a hot isostatically pressed (HIPed) pellet of ZrN. The pellet was made using —325 mesh ZrN powder (<44 μ m nominal diameter) which was HIPed in a sealed tantalum container at $T = 1850^\circ\text{C}$ and $P = 200$ MPa. This HIPing procedure resulted in a 1 by 3 inch pellet with a density near 99% theoretical density.

Figure 1 shows an optical micrograph obtained from a polished surface of one of the ZrN samples used for irradiation experiments. Grains range from approximately 10 to 50 μ m in diameter. The dark spots visible in the micrograph in Figure 1 are voids. These voids occur both within the interior of grains, as well as at boundaries and triple junctions. Figure 2 shows an X-ray diffraction (XRD) pattern obtained from a typical polished ZrN sample. Clearly, these XRD results demonstrate that the phase purity of the HIPed ZrN pellet is exceptional. It should be noted, however, that we have detected a grain boundary phase of unknown structure and composition at some interfaces between grains.

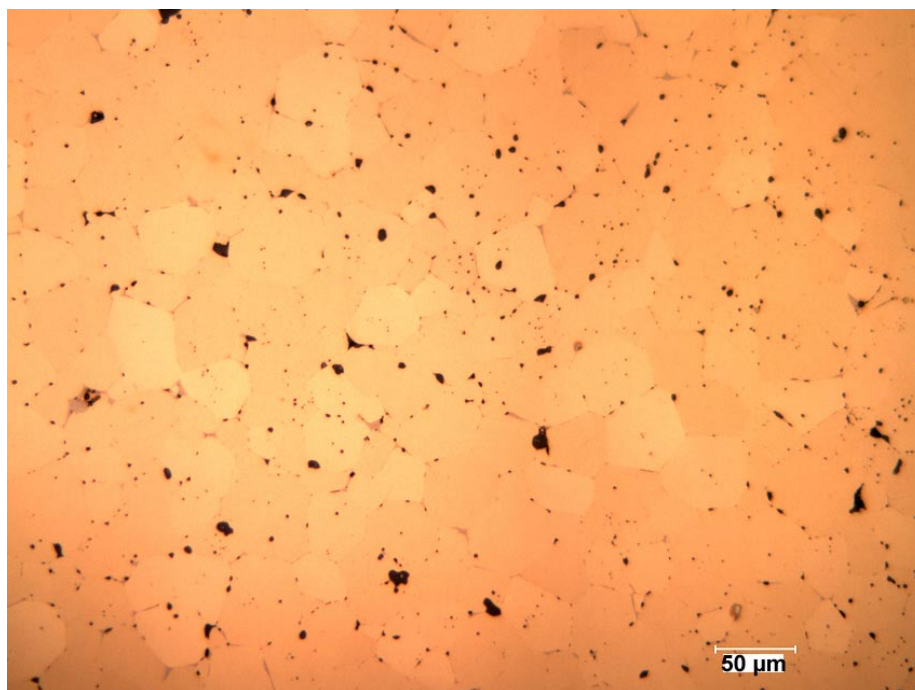


Figure 1 Optical micrograph showing the microstructure of the HIPed ZrN pellet

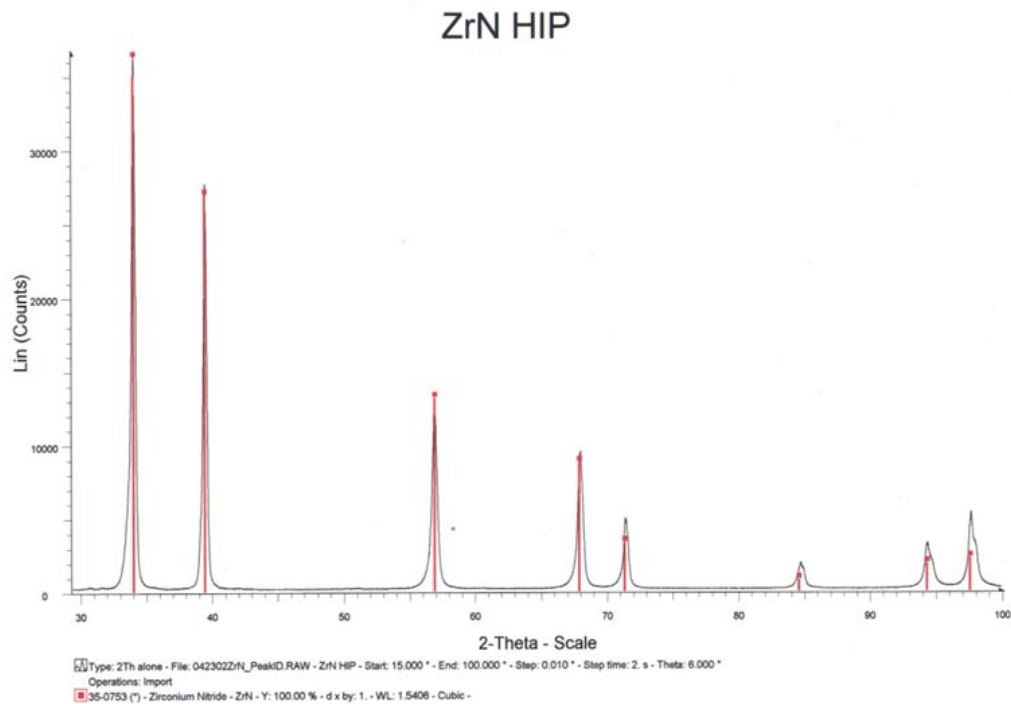


Figure 2 X-ray diffraction pattern obtained from a polished section of the HIPed ZrN pellet. Red lines indicate the scattering positions for reflections corresponding to the cubic phase of ZrN (Cu K_α radiation)

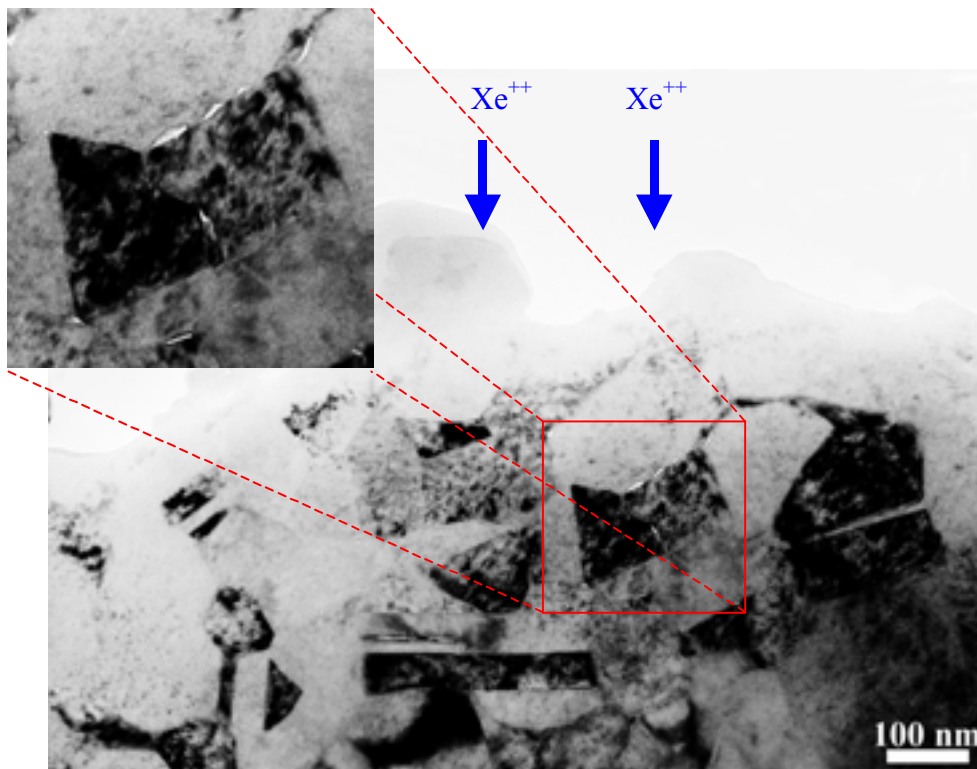


Figure 3 Voids, micro-twinning and small grains produced by 10^{16} Xe/cm³ into ZrN

Radiation Damage

TEM studies have shown that under high fluence (5×10^{16} ions/cm²) of both Xe, Kr, and He, there is some void formation at the grain boundaries (Figure 3). Grains initially are large but after irradiation the grain size is reduced by magnitudes and micro-twins have been observed. This would suggest rapid recrystallization under irradiation at temperatures as low as 100 K. Figure 3 shows an example of these effects with Xe implanted into ZrN at liquid nitrogen temperatures.

Swelling

Swelling due to inert gas implantation, either from void formation or integration into the crystal structure has not been observed. Masking was used to create an interface of implanted and non-implanted ZrN so that swelling would produce a ridge. An EDS line scan was used to show the Xe implanted area (Figure 4). Both SEM and AFM showed no change in topography at the interface where the ZrN sample had been masked.

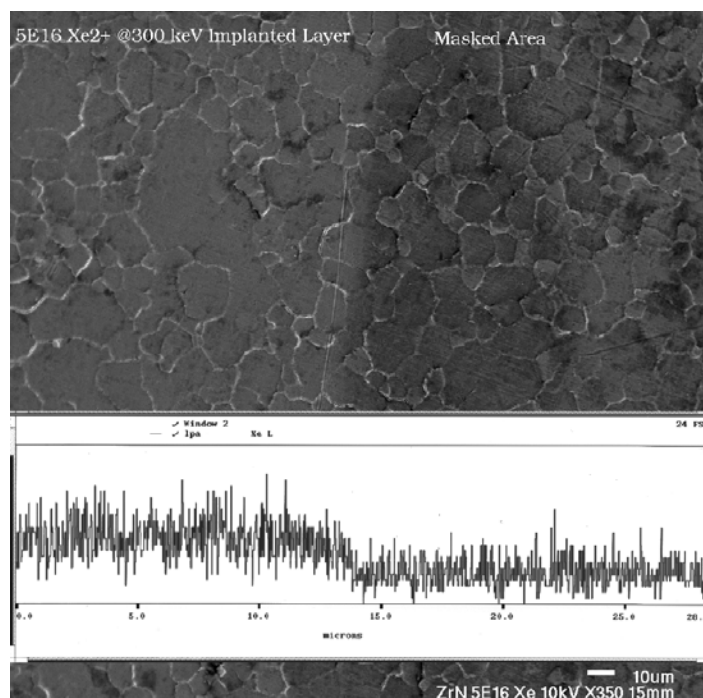


Figure 4 SEM micrograph of ZrN implanted with 5×10^{16} ions/cm² of Xe in the left ~1/2 of the sample. The inset is a concentration profile of the Xe distribution in the sample.

No swelling or uplift is associated with the high level of implanted Xe.

He Desorption Studies

ZrN samples were irradiated with Xe ions and then implanted with He ions in preparation for He release experiments. The purpose of the Xe ion irradiation was to produce a pre-existing radiation damage state in the ZrN, in order to assess the effect of radiation damage on He mobility and release. Three sets of samples were implanted with He:

- (1) pristine ZrN with no pre-existing damage;
- (2) ZrN irradiated with a low dose of Xe to produce a peak damage state of ~3.5 dpa (displacements per atom); and

(3) ZrN irradiated with a high dose of Xe to produce a peak damage state of ~35 dpa.

450 keV Xe^{3+} ions were used for the Xe ion irradiations. Ions were directed at normal incidence relative to the sample surface. This produces a peak in the ZrN displacement damage at a depth of ~500 beneath the sample surface (according to Monte Carlo simulations of ion stopping in ZrN). The peak displacement damage under these conditions is ~3.5 dpa per 10^{15} Xe/cm² unit of fluence (again based on Monte Carlo simulations). Irradiations were carried out under cryogenic conditions (substrates were maintained at T~77K). Fluences used were 1×10^{15} and 1×10^{16} Xe/cm².

13 keV He^+ ions were used for the He ion implantations. Ions were directed at 60° away from normal incidence (30° with respect to the sample surface) in order to place the peak of the He implantation profile in coincidence with the peak in the Xe ion-induced displacement damage profile (i.e., at a sample depth of ~500). Monte Carlo simulations indicate that approximately 30% of the implanted He is lost to backscattering events under these implantation conditions. All implantations were carried out at cryogenic temperature (T~100K) to a fluence of 1×10^{15} He/cm².

Figure 5 shows the ion damage profile induced by the Xe ion implantation versus depth beneath the sample surface (based on Monte Carlo computer simulations). Also shown in Figure 5 is the He ion implantation profile (also based on Monte Carlo). Experimental parameters such as ion energy and ion beam orientation were adjusted to produce the almost optimum overlap of the He ion concentration and Xe ion damage profiles shown in Figure 5.

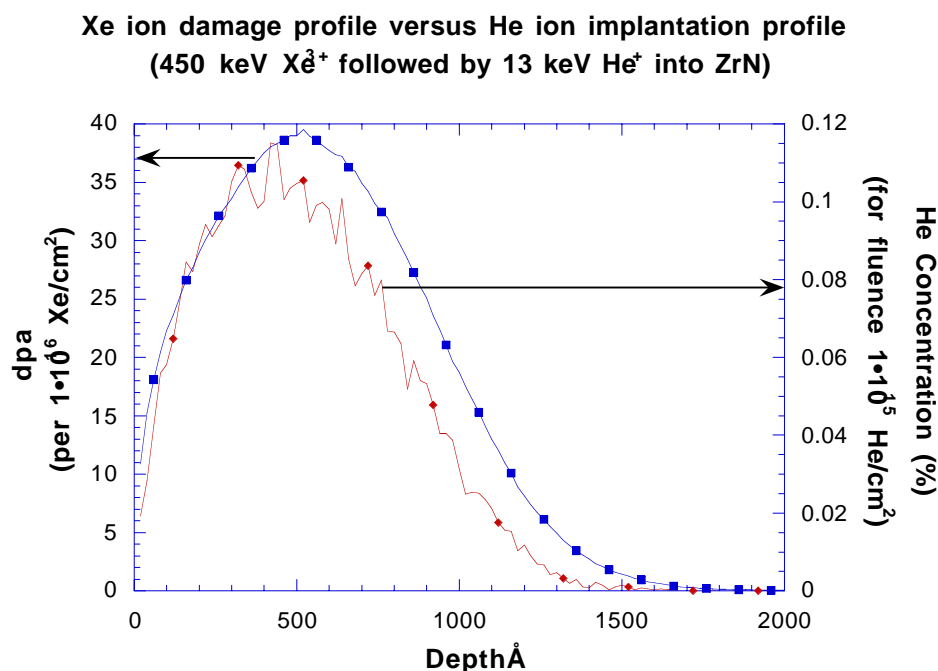


Figure 5 Blue Curve: Calculated ion damage profile induced by Xe ion implantation versus depth beneath the sample surface for an ion fluence of 1×10^{16} Xe/cm². Red Curve: Calculated He ion implantation concentration profile. For the lower fluence irradiation used in the study, 1×10^{15} Xe/cm², the values on the left-hand ordinate should be divided by 10.

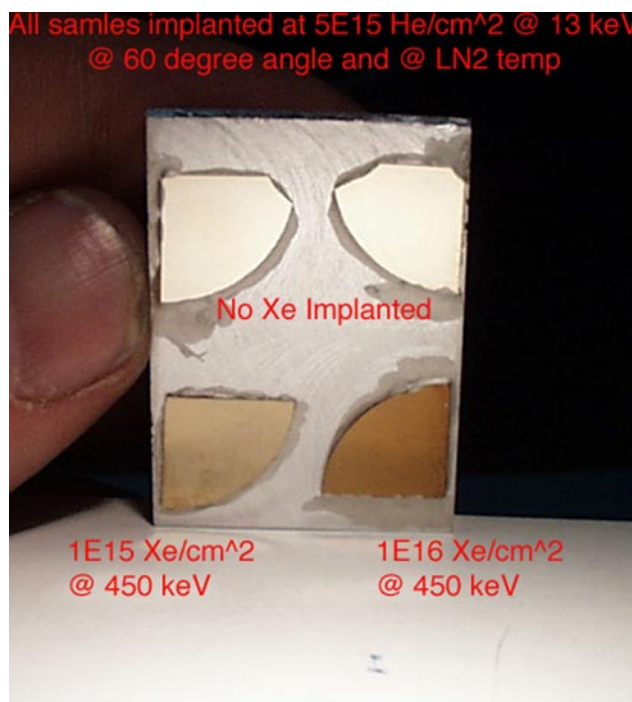


Figure 6 Photograph showing optical changes in the surface color of polished ZrN following Xe and He ion implantations to the fluences labeled.

The ion irradiated ZrN samples described above were shipped to the Institute for Transuranium Elements (ITU) in Karlsruhe, Germany for He release analyses. These samples are now with Dr. Thierry Wiss and his team. Samples will be heated in a Knudsen cell apparatus and evolution of He with time and temperature will be monitored with a residual gas analyzer. The measurements to be performed at ITU will determine the effect of pre-existing radiation damage on He trapping and He mobility in ZrN.

Figure 6 shows an optical photograph of the ZrN surfaces before and after ion irradiation. Clearly, the implantation of Xe causes a discoloration of the ZrN.

Mechanical Property Changes

Nanoindentation was performed on the HIPed samples with highly polished surfaces. The indentation tip is a small triangular diamond point that presses into the sample to depths of 200 nm. The samples were irradiated with multiple implants at different energies in the range of 10^{14} and 10^{15} Xe/cm² to produce a shelf of damage over a range of 100 nm. Individual grains were indented and averaged for statistical analysis and to exclude outliers due to anomalies such as subsurface flaws, grain boundaries, etc. Half of each sample was masked during implantation and this section was tested for direct comparison to the implanted section.

Results showed that there was a statistically significant hardening due to irradiation damage. Hardness values increases ~ 13% on a sample with a damage shelf of ~ 8 dpa. Young's modulus, however, did not significantly change, and has a value very close to the published value for a HIPed sample. Mechanical changes under irradiation can be used as a baseline for embattlement during fuel burn-up.

Nickel Aluminide (NiAl)

NiAl is a candidate metal matrix for a dispersion fuel because of its high thermal conductivity. However, it is important to consider the radiation tolerance of this intermetallic compound. Therefore, we initiated an investigation of radiation damage effects in single crystal NiAl using ion implantation followed by ion beam channeling analysis to assess the rate of radiation damage accumulation in NiAl.

Sample preparation for heavy ion damage experiments on single crystal NiAl consisted of first utilizing the back-reflection Laue technique to determine the zone axis of $\{001\}$, $\{011\}$, and $\{111\}$ NiAl to within 1.5 degrees. The orientated specimens were then cut and mechanically ground with a final polish using $1\mu\text{m}$ diamond media. A procedure for chemical milling was successfully developed to remove the remaining surface damage in the polished single crystal NiAl. The chemical milling process involved placing specimens in a chilled 5% perchloric acid, 95% ethanol solution while supplying a voltage to the specimen. Ideal parameters were found to be 40 — 45 volts at $\sim 40^\circ\text{C}$, and 30 — 35 volts at $\sim 20^\circ\text{C}$ for 15 seconds followed by a methanol rinse. The specimen was then visually inspected and the chemical milling process repeated until the desired surface finish was acquired.

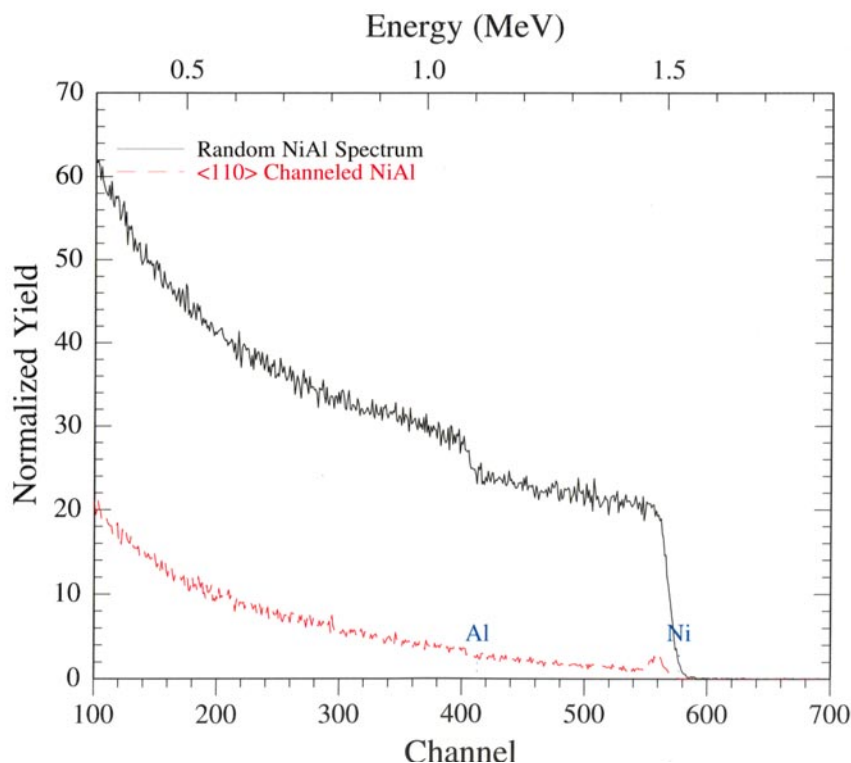


Figure 7 Red Curve: RBS/C spectrum obtained from a NiAl single crystal in a $\langle 110 \rangle$ crystallographic orientation. Black Curve: RBS spectrum obtained from the same NiAl single crystal in a random sample orientation

Crystal quality was assessed using Rutherford backscattering/ion channeling (RBS/C) analytical procedures. Figure 7 shows an RBS/C spectrum obtained from a NiAl single crystal oriented along a $\langle 110 \rangle$ crystallographic direction. Also shown in Figure 7 is an

RBS/C spectrum obtained in a random sample orientation. Crystal perfection can be qualitatively determined by measuring the ratio of the backscattered He ion yield in the channel orientation versus the yield in a random orientation. This ratio, referred to as χ_{min} , was found to be approximately 5%. This represents very high crystalline quality in comparison to single crystals of other compounds examined by this same procedure.

Conclusions

High energy, light and heavy noble gas ion irradiations were performed on high density polycrystalline samples of ZrN. The damage was assessed using various characterization techniques including electron microscopy, nanoindentation, X-ray diffraction, Rutherford backscattering/ion channeling, etc. The damage accumulation and corresponding property changes have been examined at very high ion irradiation doses. ZrN has been shown to be stable under substantial irradiation with respect to amorphization, swelling, and drastic mechanical changes.

Initial characterization of the NiAl single crystals show them to be well suited for Rutherford backscattering/ion channeling studies of radiation damage tolerance.